Electronic Supplementary Material (ESI) for Sustainable Energy & Fuels.

Supporting Information

TiO_2-Mediated Visible-Light-Driven Hydrogen Evolution by Ligand-Capped Ru Nanoparticles

Nuria Romero,[a] Renan Barrach Guerra,[b] Laia Gil,[a] Samuel Drouet,[c] Ivan Salmeron-Sànchez,[a] Ona Illa,[a] Karine Philippot,[c] Mirco Natali,[d]* Jordi García-Antón,[a]* Xavier Sala,[a]*

[a] Departament de Química, Universitat Autònoma de Barcelona, 08193-Bellaterra, Barcelona, Spain.
[b] UNICAMP - Instituto de Química, I-102, Postal box 6154 CEP 13083-970 Cidade Universitária - Campinas, SP, Brasil.
[c] LCC-CNRS, Université de Toulouse, CNRS, UPS, 205, route de Narbonne, F-31077 Toulouse, France.
[d] Dipartimento di Scienze Chimiche e Farmaceutiche, Università degli Studi di Ferrara, Via L. Borsari, 46, 44121 Ferrara, Italy.

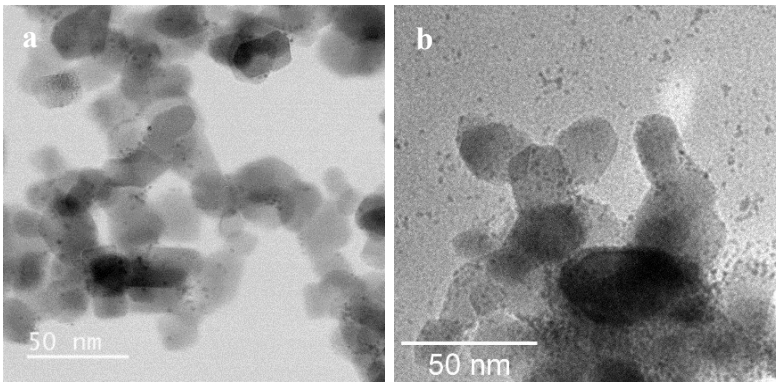

Figure S1. (a) TEM image of **RuPP(2%)-TiO_2**, (b) TEM image of **RuPP(10%)-TiO_2**.

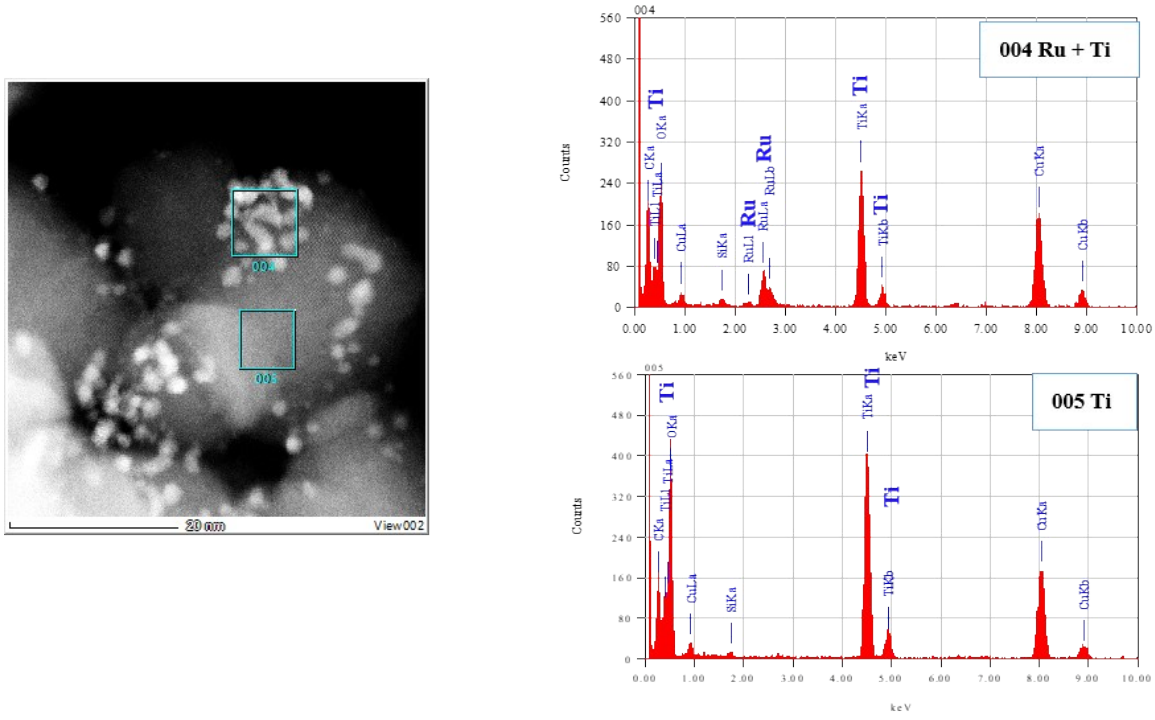

Figure S2. EDX analysis of **Ru@RuO_2PP-TiO_2**

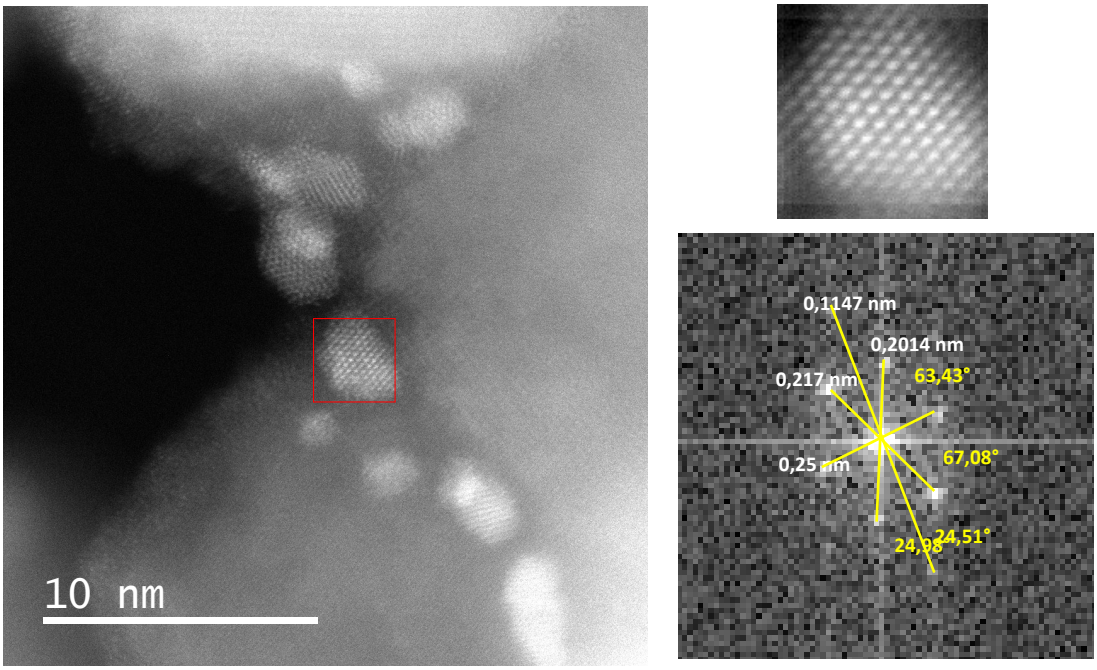

Figure S3. HRTEM of **Ru@RuO_2PP-TiO_2** at atomic resolution and Fast Fourier Transformation of the electron diffraction pattern.

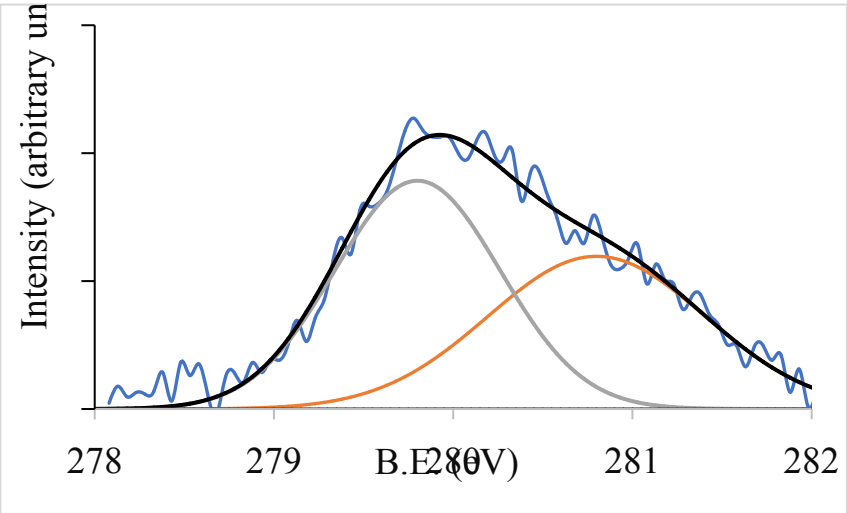

Figure S4. XPS analysis of **Ru@RuO_2PP-TiO_2**.

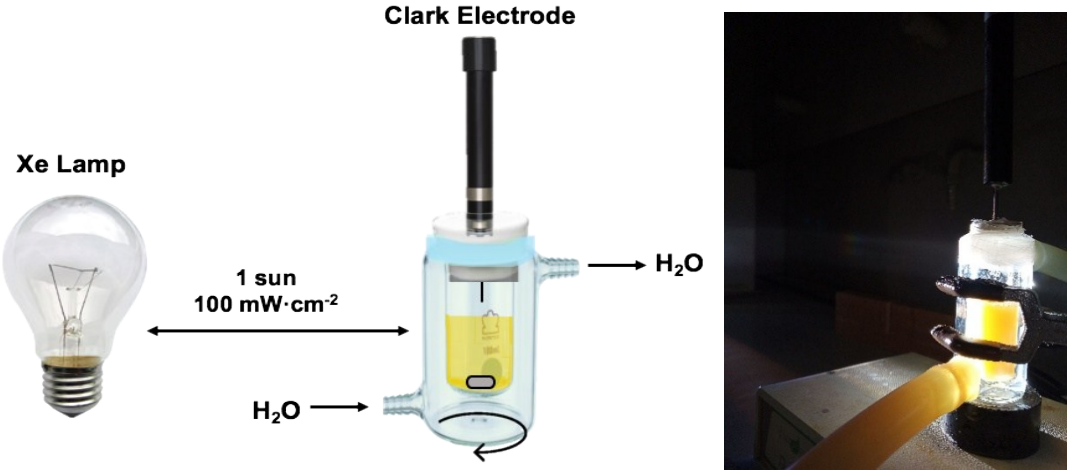

Figure S5. Schematic representation of the photocatalytic setup and picture.

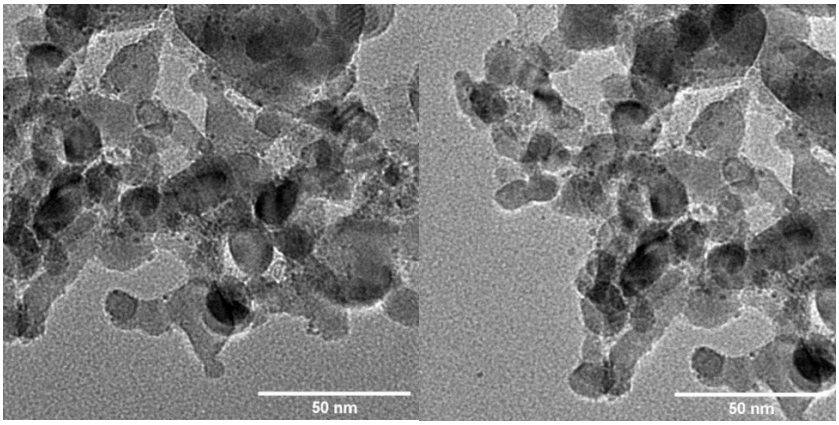

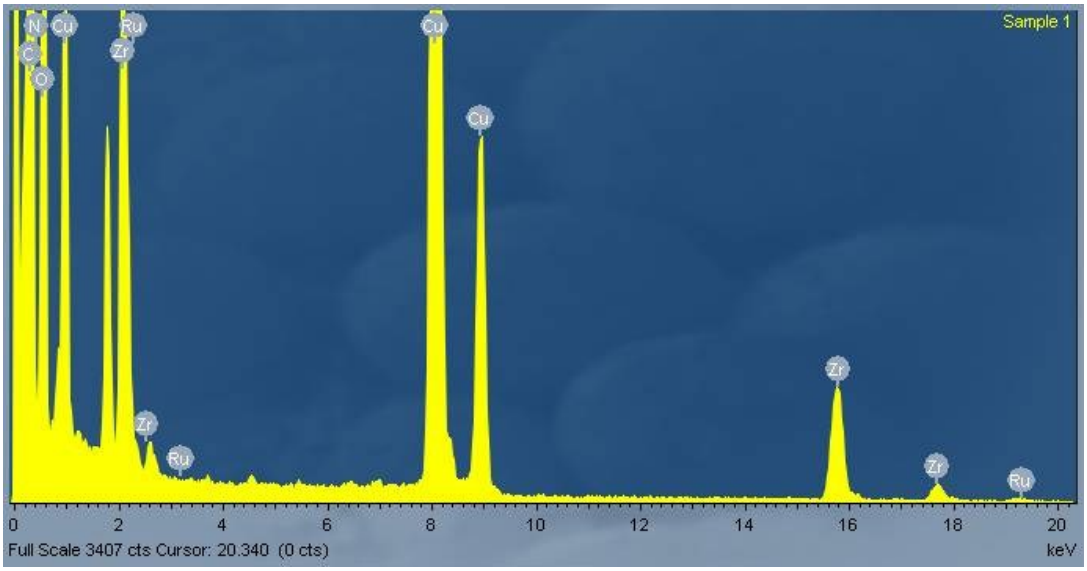

Figure S6. TEM and EDX analysis of **Ru@RuO_2PP-ZrO_2**.

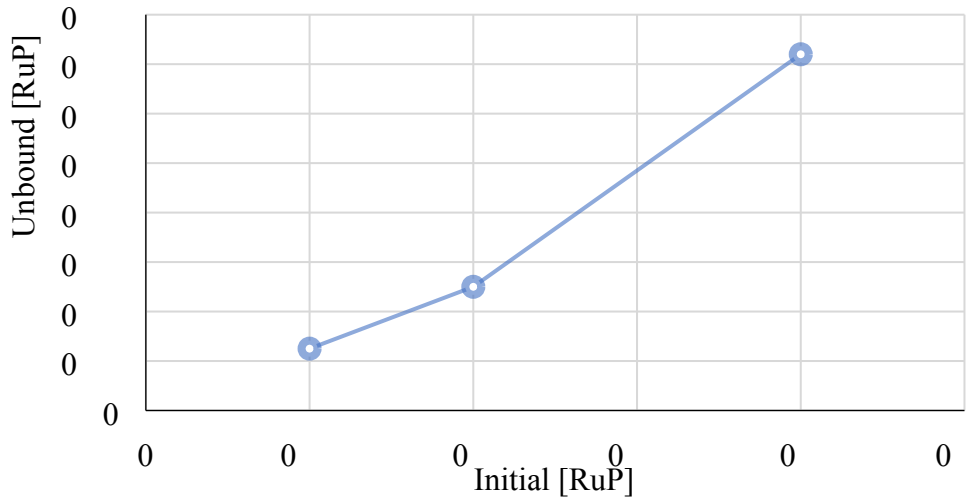

Figure S7. Evolution of the unbound [RuP] along the 0.05-0.2 mM range studied.

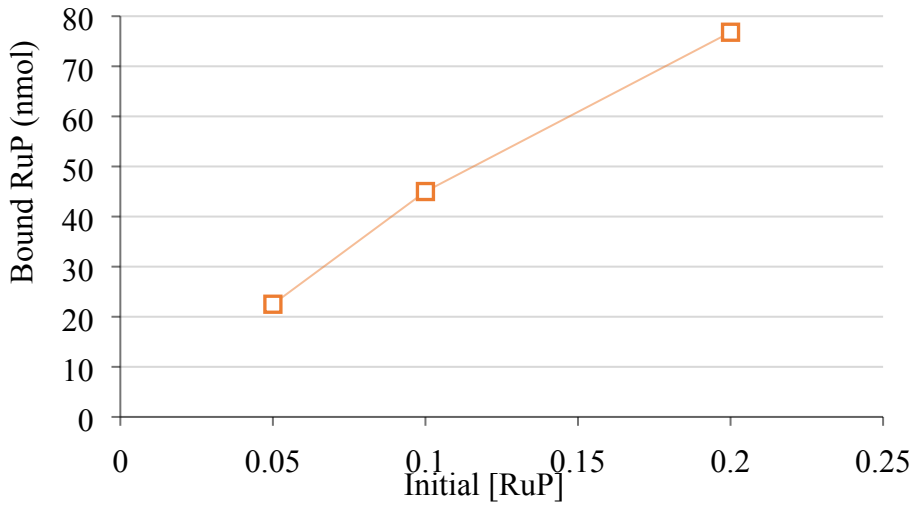

Figure S8. Evolution of the bound RuP along the 0.05-0.2 mM range studied.

(a)

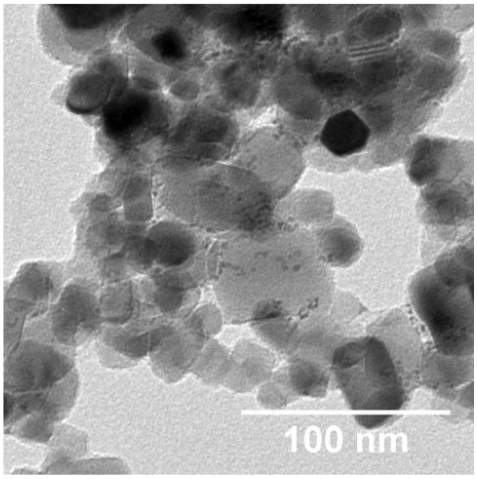

(b)

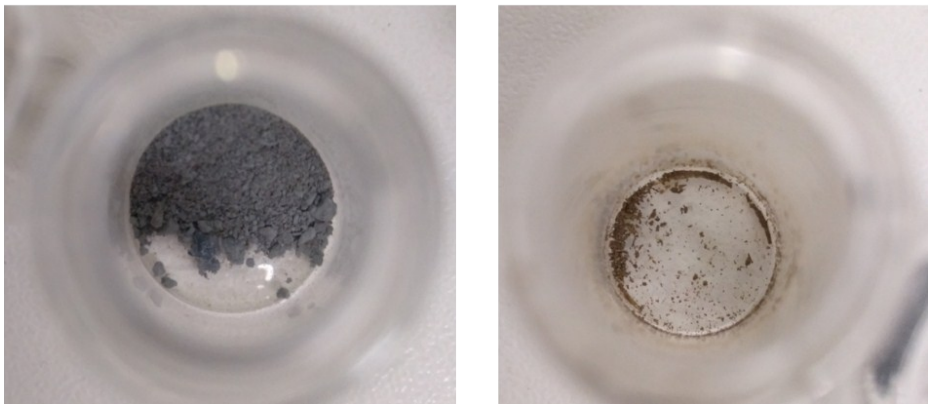

Figure S9. (a) TEM Image of **Ru@RuO$_2$PP-TiO$_2$-RuP**. (b) Color change from **Ru@RuO$_2$PP-TiO$_2$** (left) to **Ru@RuO$_2$PP-TiO$_2$-RuP** (right).

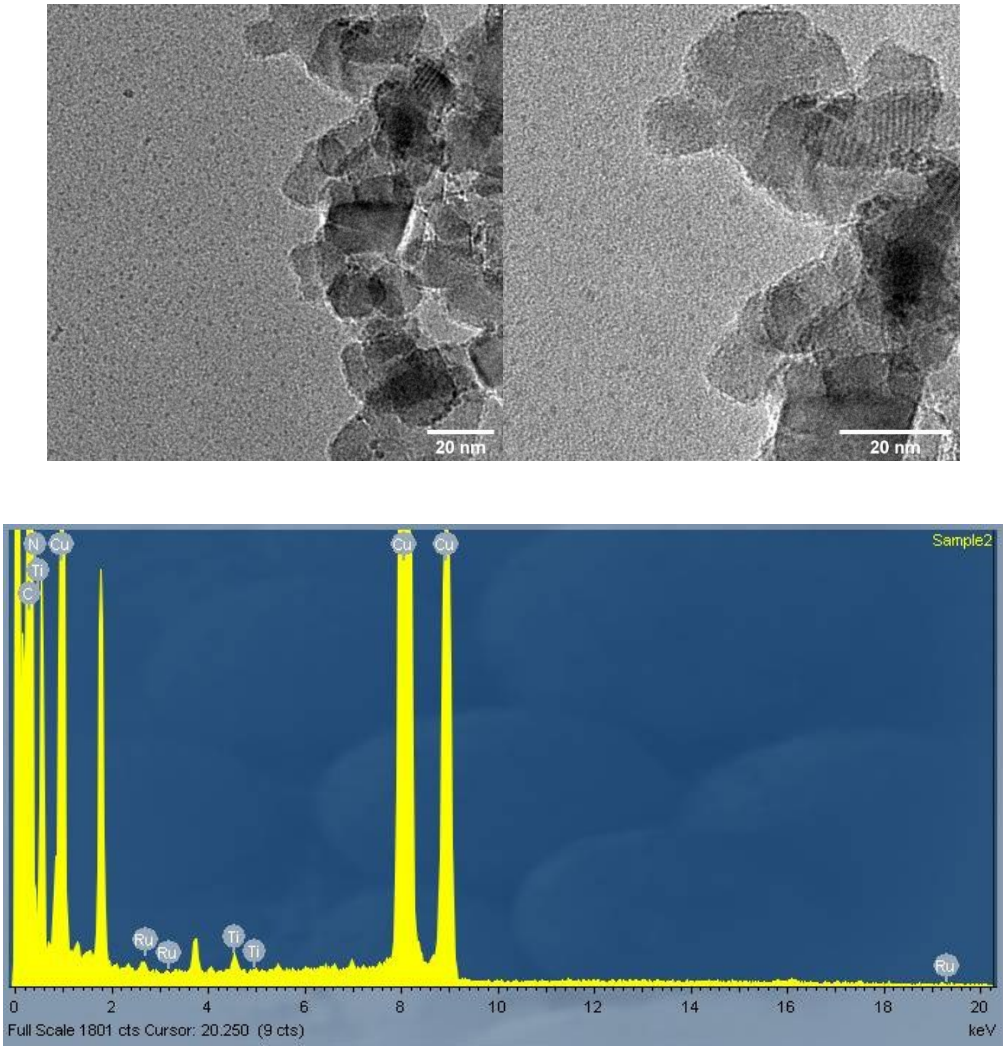

Figure S10. Top: TEM of **Ru@RuO$_2$PP-TiO$_2$** + RuP at the end of photocatalytic hydrogen evolution containing free and supported **Ru@RuO$_2$PP** NPs. Bottom: EDX outside the TiO_2 particles.

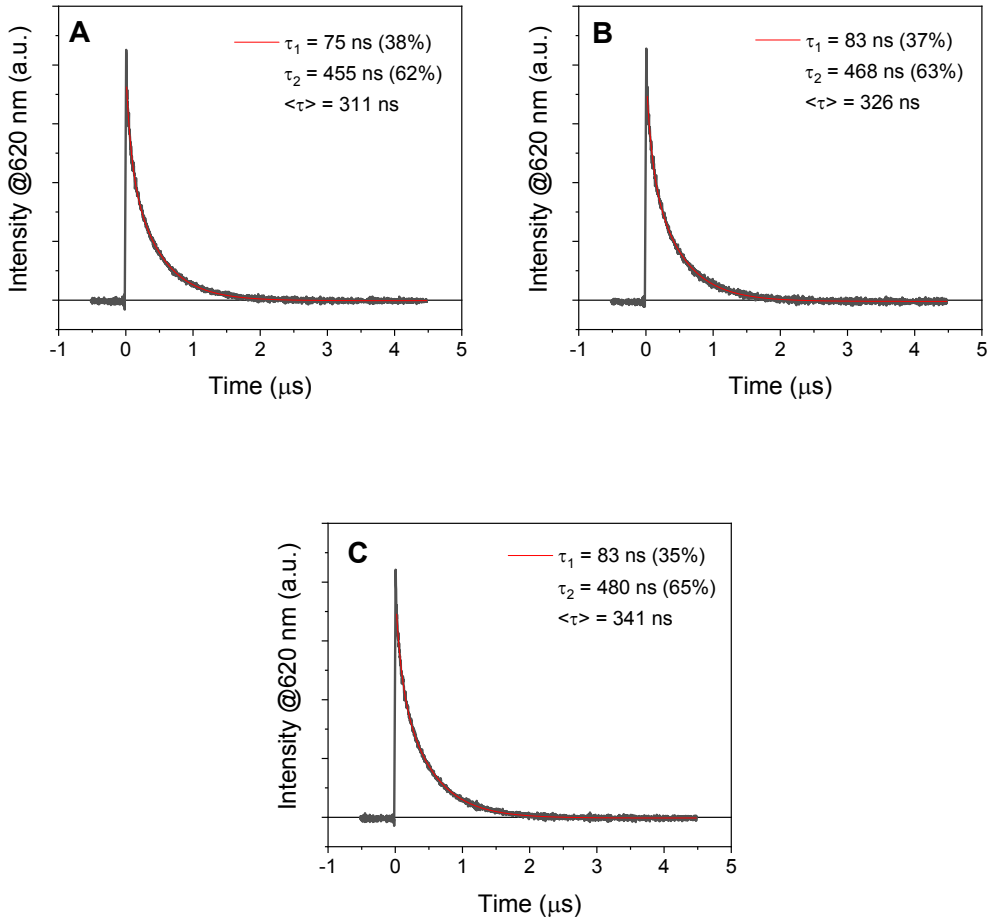

Figure S11. Time-resolved luminescence decays with related biexponential fitting measured at 620 nm by laser flash photolysis (excitation at 532 nm) of thin films in N_2-purged aqueous solutions: (A) RuP on ZrO_2 in 0.1 M Na_2SO_4 at pH 7, (B) RuP and Ru@RuO_2PP on ZrO_2 in 0.1 M Na_2SO_4 at pH 7, and (C) RuP on ZrO_2 in 0.2 M TEOA at pH 7 (blue trace).

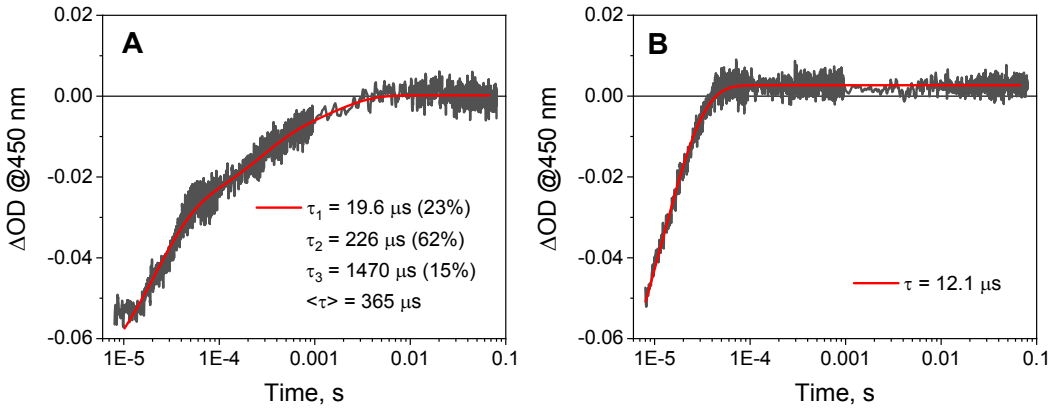

Figure S12. Transient absorption kinetics at 450 nm with related fitting measured by laser flash photolysis (excitation at 532 nm) of RuP on TiO_2 thin films in N_2-purged aqueous solutions containing (A) 0.1 M Na_2SO_4 at pH 7 and (B) 0.2 M TEOA at pH 7.

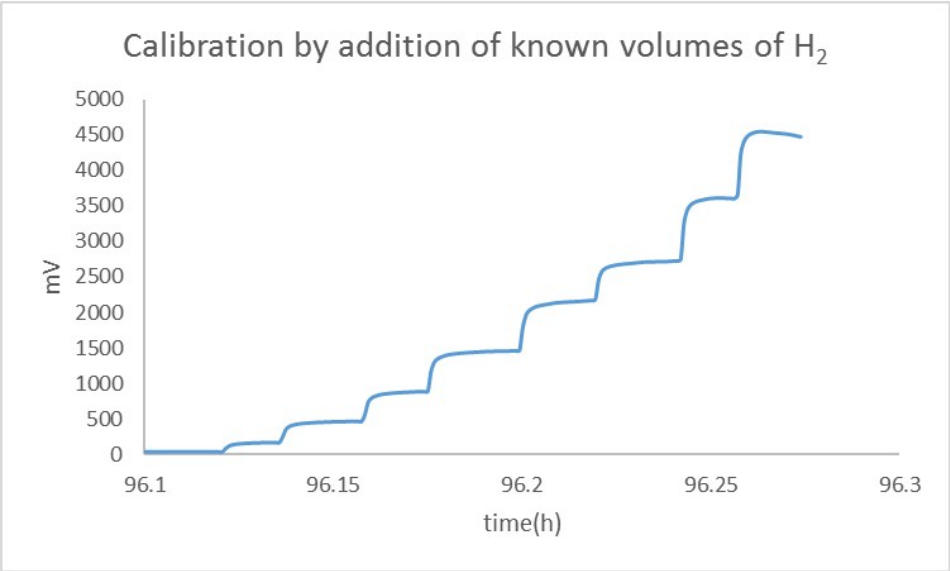

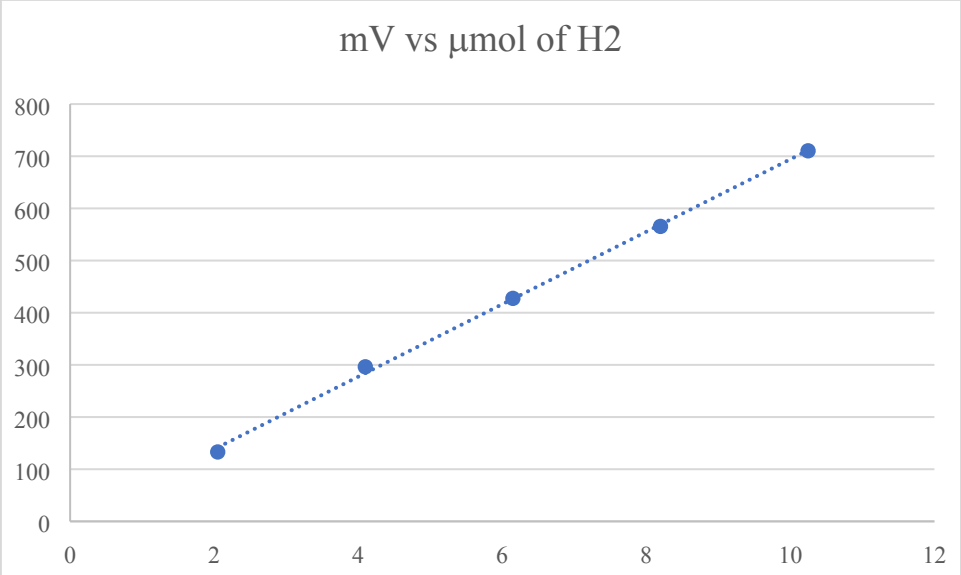

Figure S13. Example of calibration of the Clark electrode signal performed after one experiment by addition of 50, 100, 150, 200, 250, 300, 350 and 400 µl of H_2. Volume to mols conversion is performed following the general gas law equation PV = nRT.

Table S1. Photocatalytic HER data of **Ru@RuO_2PP-TiO_2-RuP** and related TiO_2-supported photocatalysts. Values in bold are explicitly cited in the corresponding articles. Others are estimated from HE plots and other reported data.

Entry	Material	μmol M	SED	Cell (solution vol.)	Irradiation	PS	μmol H_2 (max.time reported)	TOF $_{3h}$ (h^{-1})	HE_{MAX} rate (μmol_{H2} h^{-1} g_{cat}^{-1})	Ref.
1	Ru@RuO_2PP-TiO_2 (P25)-RuP	0.63	TEOA 0.2M pH 7	glass, 25ºC (4 ml)	1 sun, Xe, λ> 400 nm	RuP 0.0076m M	281 (122h)	16	3150	This work
2	Ru^0RuO_2 (8%)/TiO_2 NB-400	7.92	$EDTANa_2$ 0.01g/mL	quartz pyrex (10 ml)	300 W Xe, UV-vis	TiO_2	900 (5h)	374	**25**	1
3	PtNPs/TiO_2	0.77	10 % v/v TEOA pH 7	pyrex (20 ml)	1 sun, UV-vis	Zn phth. 12.5 μM, TiO_2	**2260 (5h)**	587.84	-	2
4	Pt NPs/TiO_2	-	30% v/v TEOA	glass, (10 ml)	150W Xe, UV-vis	TiO_2	40 (6h)	-	1000	3
5	Nafion-Pt NPs/TiO_2 anatase	0.26	10 % v/v TEOA pH 7	pyrex, (20ml)	400 W Xe, λ>400nm	MK2 10^{-4} mol	**566.9 (6h)**	442.18	9440	4
6	EosinY-Pt NPs/TiO_2	-	10% v/v TEOA	(3ml)	200 W Xe, λ>420nm	Eosin Y	**102 (20h)**	-	2500	5
7	MK2-Pt NPs/TiO_2	-	TEOA 0.33M, pH 9	Pyrex glass (<135 ml)	Solar, λ>420 nm,	MK2 10^{-4} mol	**18590 (8h)**	-	**1828**	6
8	UP3-Pt NPs/TiO_2 anatase	0.51	TEOA 10%, pH 7	pyrex glass (20 ml)	300 W Xe, λ>420 nm	UP3 1.5 μmol	4098 (60h)	266.61	10480	7
9	GS12-Pt NPs/TiO_2 anatase	0.51	TEOA 10%, pH 7	pyrex glass (20 ml)	2 sun, 400 W Hg	GS12 0.25 μmol/g, TiO_2	2820 (24h)	344.64	10500	8
10	LG5-Pt NPs/ HP-TiO_2	0.513	TEOA 2ml pH 7	pyrex (20 ml)	2 sun, 450 W Xe	LG5 5 μmol/g, TiO_2	357 (50h)	21.46	**4196**	9
11	Pt NPs/TiO_2	0.19	EDTA 10mM pH 3	(25 ml)	450W Xe, 10^{-3} E/(L min), 420 nm<λ< 500 nm	RuP 10 μM	**130 (3h)**	225.43	-	10,11
12	PtNPs/TiO_2	0.08	EDTA 10mM, PO_4^{3-} 500μM, pH 4	glass, (30 ml)	300 W Xe, λ>420 nm	$[Ru(bpy)_3]^{2+}$ 30μM	20 (4h)	65.03	333	12
13	$RuCP^2$-phen-Zr-RuP^6@Pt-TiO_2 anatase	0.12	L-ascorbic acid 20 ml, pH 4	quartz, 20ºC (5ml)	blue LED lamp, λ= 470 nm	$RuCP_2$-phen-Zr-RuP_6 100 μM, TiO_2	100 (3h)	**143.00**	-	13
14	4(bpy)P-Pt NPs/TiO_2	0.51	L-ascorbic acid 0.5 M, pH 4	vial 15ºC (5ml)	LED 130mW, 530 nm	4(bpy)P 0.125 mol	4903 (288h)	-	2541	14
15	Dy1-PtNPs/TiO_3	0.51	L-ascorbic acid 0.5 M, pH 4	vial 15ºC (5ml)	700 LEDs 130mW 410-800 nm	Dy1 0.125 mol	482 (60h)	-	614	15
16	PtRDMI3-PtNPs/TiO_2	0.51	L-ascorbic acid 0.5 M, pH 4	vial 15ºC (5ml)	700 LEDs 130mW 400-800 nm	PtRDMI3 0.125 mol	**4900(80h)**	-	6000	16
17	YD2-o-C8-Pt NPs/TiO_2	0.51	L-ascorbic acid 0.5 M, pH 4	vial 19ºC (5ml)	700 LEDs 80mW 420-800 nm	YD2-o-C8 0.125 mol	798 (120h)	-	**1360**	17
18	CoP	0.08	TEOA 0.1M pH 7	25ºC (4.5 ml)	100 mW/cm^2, λ>420nm	RuP 0.1 μmol	(10h)	-	**600**	18
19	NiP complex /RuP /TiO_2 P25	0.02	Ascorbic acid	25ºC, (2.25 ml)	100 mW/cm^2, λ>420nm	RuP 0.05 μmol	**1.7 (2h)**	-	0.41	11,19
20	NiP complex /RuP	4.50	Ascorbic acid	25ºC, (2.25 ml)	100 mW/cm^2, λ>420nm	RuP 0.05 μmol	**14.5 (2h)**	-	-	11,19

Table S2. Photocatalytic HER data of nanoparticulated Ru- or Pt-based non-supported photocatalysts. Values in bold are explicitly cited in the corresponding articles. Others are estimated from HE plots and other reported data.

Entry	Material	μmol M	SED	Cell (volume of solution)	Irradiation	PS	μmol H_2 (maximum time reported)	HE_{MAX} rate (μmol_{H2} h^{-1} g_{cat}^{-1})	Ref.
1	Ru@RuO_2PP	0.01	TEOA 0.2M pH 7	glass, 25ºC (4 ml)	1 sun, Xe, λ> 400 nm	RuP 0.1 mM	0	0	This work
2	Ru PVP NPs	2.47	phthalate buffer pH 4.5 + MeCN 1:1, NADH 1 mM	quartz, (2 ml)	Xe, λ>340nm,	$QuPh^+$-NA 0.88 mM	2 (4 min)	1160	20
3	Pt PVP NPs	1.28	phthalate buffer pH 4.5 + MeCN 1:1, NADH 1 mM	quartz, (2 ml)	Xe, λ>340 nm,	$QuPh^+$-NA 0.22 mM	2 (4 min)	1200	20
4	Pt NPs	1.69	TEOA 0.2M, pH 7	pyrex (10ml)	200 W halogen, λ>400 nm	$[Ru(bpy)_3]^{2+}$ 91 mM + $[Rh(bpy)_3]^{3+}$ 1.95 mM	-	350000	21

Estimation of the apparent quantum yield (AQY)

The AQY (%) was estimated under optimized conditions from the ratio between the rate of hydrogen production (R_{H_2} = 3.5·10^{-9} mol·s^{-1}, corresponding to the value of 12.6 μmol·h^{-1} experimentally determined, see main text) and the absorbed photon flux (Φ_{ABS} = 2.67·10^{-7} einstein·s^{-1}), according to eq S1.

$$AQY\ (\%) = \frac{R_{H_2}}{\Phi_{ABS}} \qquad \text{(S1)}$$

The absorbed photon flux (Φ_{ABS}) has been estimated according to eq. S2,

$$\Phi_{ABS} = A \cdot \int P_{AM1.5G} \cdot \left(1 - 10^{-\varepsilon_\lambda l[RuP]}\right) d\lambda \qquad \text{(S2)}$$

where A is the irradiated surface area (0.00053 m^2), $P_{AM1.5G}$ is the spectral irradiance of the Sun at the Earth's surface (einstein·s^{-1}·m^{-2}·nm^{-1}), ε_λ (M^{-1}·cm^{-1}) is the absorption spectrum of the RuP chromophore in water in the irradiated wavelength range considering that a cut-off filter with λ > 400 nm has been used, l is the optical pathlength (0.9496 cm, estimated as the average value considering the cylindrical geometry of the reactor and the diameter of 1.5 cm), [RuP] = 7.6·10^{-5} M is the concentration of the

chromophore attached onto TiO_2 in the photocatalytic experiment under optimized conditions (see main text).

Pictorial representation of the incident photon flux ($P_{AM1.5G}$) and absorbed photon flux per surface area (Φ_{ABS}/A) used for the calculation of the AQY is reported in Figure S14.

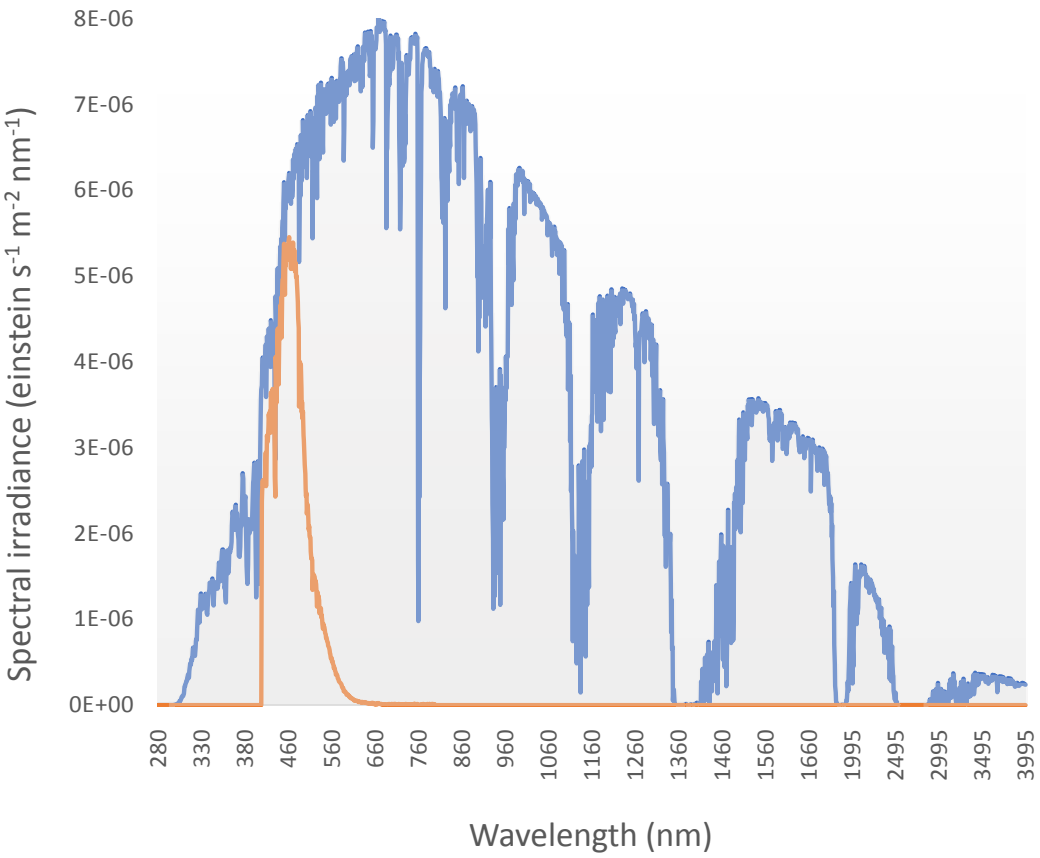

Figure S14. Spectral irradiance of the Sun at the Earth's surface ($P_{AM1.5G}$, blue line) and absorbed photon flux per surface area (Φ_{ABS} /A, orange line) under the optimized experimental conditions for hydrogen evolution with the **Ru@RuO_2PP-TiO_2-RuP** hybrid.

References

1 Q. Gu, Z. Gao, S. Yu and C. Xue, *Adv. Mater. Interfaces*, 2016, **3**, 1500631.

2 A. Tiwari, N. V. Krishna, L. Giribabu and U. Pal, *J. Phys. Chem. C*, 2018, **122**, 495–502.

3 I. Mondal, S. Gonuguntla and U. Pal, *J. Phys. Chem. C*, 2019, **123**, 26073–26081.

4 A. Kumari, I. Mondal and U. Pal, *New J. Chem.*, 2015, **39**, 713–720.

5 J. H. Park, K. C. Ko, N. Park, H.-W. Shin, E. Kim, N. Kang, J. Hong Ko, S. M. Lee, H. J. Kim, T. K. Ahn, J. Y. Lee and S. U. Son, *J. Mater. Chem. A*, 2014, **2**, 7656.

6 E. Aslan, M. Karaman, G. Yanalak, H. Bilgili, M. Can, F. Ozel and I. H. Patir, *J. Photochem. Photobiol. A Chem.*, 2020, **390**, 112301.

7 A. Tiwari, I. Mondal and U. Pal, *RSC Adv.*, 2015, **5**, 31415–31421.

8 T. Swetha, I. Mondal, K. Bhanuprakash, U. Pal and S. P. Singh, *ACS Appl. Mater. Interfaces*, 2015, **7**, 19635–19642.

9 S. Gonuguntla, A. Tiwari, S. Madanaboina, G. Lingamallu and U. Pal, *Int. J. Hydrogen Energy*, 2020, **45**, 7508–7516.

10 E. B. And and W. Choi, *J. Phys. Chem. B*, 2006, **110**, 14792–14799.

11 J. Willkomm, K. L. Orchard, A. Reynal, E. Pastor, J. R. Durrant and E. Reisner, *Chem. Soc. Rev.*, 2016, 45, 9–23.

12 C. Park, J. J. Park, J. J. Park, I. Heo, W. Kim and J. Kim, *Catal. Today*, 2019, **335**, 236–242.

13 N. Yoshimura, A. Kobayashi, M. Yoshida and M. Kato, *Bull. Chem. Soc. Jpn.*, 2019, **92**, 1793–1800.

14 B. Zheng, R. P. Sabatini, W. F. Fu, M. S. Eum, W. W. Brennessel, L. Wang, D. W. McCamant and R. Eisenberg, *Proc. Natl. Acad. Sci. U. S. A.*, 2015, **112**, E3987–E3996.

15 P. Y. Ho, B. Zheng, D. Mark, W. Y. Wong, D. W. McCamant and R. Eisenberg, *Inorg. Chem.*, 2016, **55**, 8348–8358.

16 G. Li, M. F. Mark, H. Lv, D. W. McCamant and R. Eisenberg, *J. Am. Chem. Soc.*, 2018, **140**, 2575–2586.

17 P. Ho, M. F. Mark, Y. Wang, S. Yiu, W. Yu, C. Ho, D. W. McCamant, R. Eisenberg and S. Huang, *ChemSusChem*, 2018, **11**, 2517–2528.

18 F. Lakadamyali, A. Reynal, M. Kato, J. R. Durrant and E. Reisner, *Chem. - A Eur. J.*, 2012, **18**, 15464–15475.

19 M. A. Gross, A. Reynal, J. R. Durrant and E. Reisner, *J. Am. Chem. Soc.*, 2014, **136**, 356–366.

20 Y. Yamada, T. Miyahigashi, H. Kotani, K. Ohkubo and S. Fukuzumi, *J. Am. Chem. Soc.*, 2011, **133**, 16136–16145.

21 M. Kirch, J.-M. Lehn and J.-P. Sauvage, *Helv. Chim. Acta*, 1979, **62**, 1345–1384.